한국가시화정보학회지, 제7권, 제2호, (2010) 35~41
<일반논문> (투고일: 2009.11.23/수정일: 2009.12.30/심사완료일: 2009.12.30)

초음속 마이크로제트 유동의 수치해석적 가시화

신춘식* · 이종성* · 김희동†

Numerical Visualization of Supersonic Microjet Flows

Choon Sik Shin, Jong Sung Lee and Heuy Dong Kim

Abstract. Supersonic microjets acquire considerable research interest from a fundamental fluid dynamics perspective, in part because the combination of highly compressible flow at low-to-moderate Reynolds number is not very common, and in part due to the complex nature of the flow itself. In addition, micro-jets have a great variety engineering applications such as micro-propulsion, MEMS(Micro-Electro Mechanical Systems) components, microjet actuators and fine particle deposition and removal. Numerical simulations have been carried out at moderate nozzle pressure ratios and for different nozzle exit diameters to investigate and to understand in-depth of aerodynamic characteristics of supersonic microjets.

Key Words: Compressible Flow(압축성 유동), Microjets(마이크로제트), Supersonic(초음속), Jet Structure (제트 구조), Numerical Simulation(수치 시뮬레이션)

1. Introduction

Microjets acquire considerable research interest due to their potential use in various engineering applications such as micro-propulsion, MEMS components, and fine particle deposition and removal. Supersonic microjets provide several advantages over subsonic jets in a number of applications. Microjets are also used as actuators to control the ground effect created by large supersonic impinging jets, typically occur in STOVL (Short Take-off and Vertical Landing) aircraft during hover. More recently, micro-jet actuators have also been used for controlling the flow separations, cavity flows, jet noise, and for suppressing turbulence in jet flows. In addition, the flowfield of microjets is also of interest from a fundamental fluid dynamics perspective, in part because the combination of highly compressible flow at low-to-moderate Reynolds number is not very common, and in part due to the complex nature of the flow itself.

To-date most studies involving fluid flows at microscales have mainly focused on internal flows in nozzles and micro-channels. Meinhart et al.[1] describe a MicroPIV investigation of flow through an inkjet printer. A detailed computational and experimental study examining the flowfield inside silicon-etched converging-diverging (c-d) micro-nozzles with throat heights ranging from 10~50 mm was carried out by Breuer and Bayt[2]. The study underlined the behavior and influence of the nozzle boundary layer on the thrust performance of these micronozzles. No measurements of the external flow were made in their work, the presence of supersonic flow was estimated via mass flow and thrust measurements. Scroggs and Settles[3] fabricated micronozzles by heating and stretching glass capillaries. Using this method, they fabricated converging-diverging nozzles and obtained schlieren images and pitot pressure surveys along the centerline for supersonic jets issuing from the c-d nozzles, ranging in size from 600 mm to 1,200 mm. Smedley et al.[4] discuss an application of supersonic microjets for surface

†School of Mechanical Engineering, Andong National University
E-mail: kimhd@andong.ac.kr
*School of Mechanical Engineering, Andong National University

entrainment of particles for shock induced cleaning. Krothapalli et al.[5] described a micro-schlieren system with a large magnification to visualize the flowfields qualitatively. More recently, Vela´squez-Aguilar et al.[6] applied the dual-hologram techniques to measure the same phase object by reference beam and shear techniques using only three Mach-Zehnder holograms: one comparison hologram and two identical signal ones. In most recent, Phalnikar et al.[7] conducted experiments on free and impinging supersonic microjets using micro-schlieren system and through pitot pressure measurements. Since, the numerical simulation is an extremely important and most widely used tool to analyze and understand the in-depth of fluid flow behaviors. Moreover, till date, no considerable numerical work has been done to investigate the aerodynamic behavior of supersonic microjets.

Therefore, it requires performing numerical investigation the aerodynamic characteristics of supersonic microjets.

The present study pertains with numerical simulations of supersonic microjets at moderate nozzle pressure ratios. Especially, we focused on the effect of nozzle exit diameter on the aerodynamic characteristics of microjets.

2. Numerical Approaches

The two-dimensional viscous flow solver, developed at our laboratory, is used for these computations. It is based on the compressible Reynolds and Favre-averaged Navier-Stokes equations, and modified Goldberg's[8] k-γ turbulence model is used for closure. The governing equations are non-dimensionalized with reference values at the inlet conditions upstream of the nozzle written in an axisymmetric coordinate system. The 3rd order TVD (Total Variation Diminishing) finite difference scheme with MUSCL approach[9] is used to discretize the spatial derivatives, a second order-central difference scheme for the viscous terms, and a second-order fractional step is employed for time integration.

3. Computational Conditions

Axisymmetric supersonic microjets flow driven by the sonic nozzle[10] with exit diameters of D_e = 400 μm, 200 μm and 100 μm (characteristic length) are considered in the present computation, as shown in Fig. 1. The dry air as working gas is issued from that sonic nozzle. The structured clustered grids are used for these computations to obtain reasonable solutions in a flow with large pressure and velocity gradient. Several tests are conducted to select a suitable grid for obtaining grid-independent solutions. The resulting number of grids applied is 50×60 in the nozzle region and 200×111 in the jet plume region.

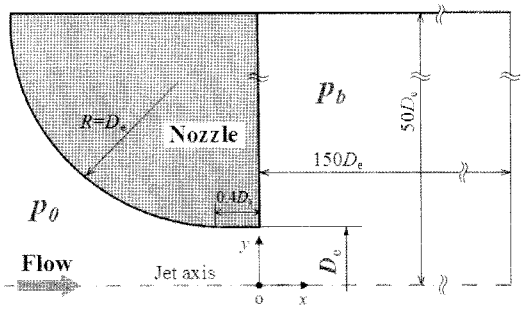

Fig. 1. Computational domain

In this present study, three nozzle pressure ratios ($=p_0/p_b$), the ratio of the reservoir pressure p_0 (atmospheric pressure) to back pressure p_b, used are 4.57, 5.23 and 6.2, respectively. Total temperature T_0, total pressure p_0 in the reservoir are 298.15 K, 101.3 kPa, respectively.

At the inflow boundary upstream of the nozzle, all variables are fixed at the initial values and all variables are extrapolated at the outflow boundary downstream of nozzle. The non-slip wall condition is used on the solid surface. The axisymmetric condition is used at the boundary of the nozzle centre line. Iso-pressure and no heat transfer are constrained on the solid wall.

4. Results and Discussion

4.1 Comparison with Experimental Results

The comparisons of predicted iso-density contour with schlieren photograph obtained by experiment for p_0/p_b = 6.2, is shown in Fig. 2. The sonic nozzle[10] with exit diameters of D_e = 12.7 mm are used in the computation and experiment. The jet is underexpanded at the nozzle exit and barrel shocks

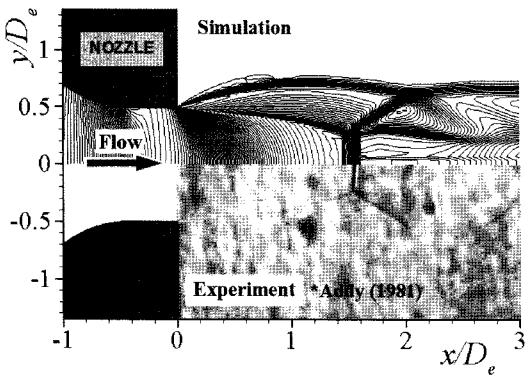

Fig. 2. Comparison of the present computation with experiment ($p_0/p_b = 6.2$)

are formed due to the differences in pressure between the underexpanded gas and the ambient gas. Therefore, these shocks reflect from the jet axis. Consequently the Mach disk is formed near the jet axis. At the intersection of the Mach disk with the barrel shock, a triple-point is formed. In the downstream of the triple-point the slip line is observed. The predicted iso-density contour is nearly same as the experimentally visualized result.

Furthermore, the predicted Mach disk location L_m and diameter L_m are $L_m/D_e = 1.5613$ and $D_m/D_e = 0.5394$, respectively, while the experimental values are 1.5646 and 0.5264, respectively. Here, location of Mach disk is measured from the nozzle exit, and both the location and diameter of the Mach disk are normalized by nozzle exit diameter. Thus, the present computational works predict well the flow structures of the highly underexpanded supersonic jets.

4.2 Structure of Supersonic Microjets

Computer schlieren images of the supersonic underexpanded jets from the nozzle with 100 μm of exit diameter at pressure ratios of 4.57, 5.23 and 6.2 are shown in Fig. 3(a-c). Similarly, Figs. 4(a-c) and 5 (a-c) show the flowfields for the 200 μm and 400 μm, respectively. In these figures, the jet flowfields evolve from weak underexpansion to strong underexpansion.

An increase in the nozzle pressure ratio makes the streamwise extent of the shock cells that roughly indicated increased length of the 'supersonic core'. This trend has also been depicted for

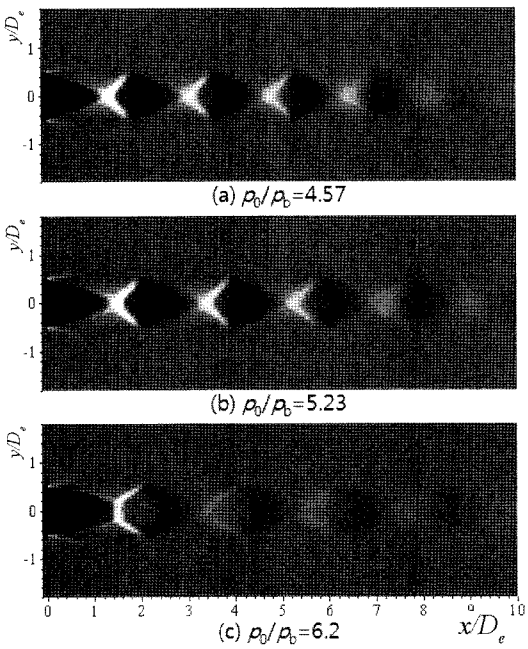

Fig. 3. Numerical schlieren images of 100 μm microjets

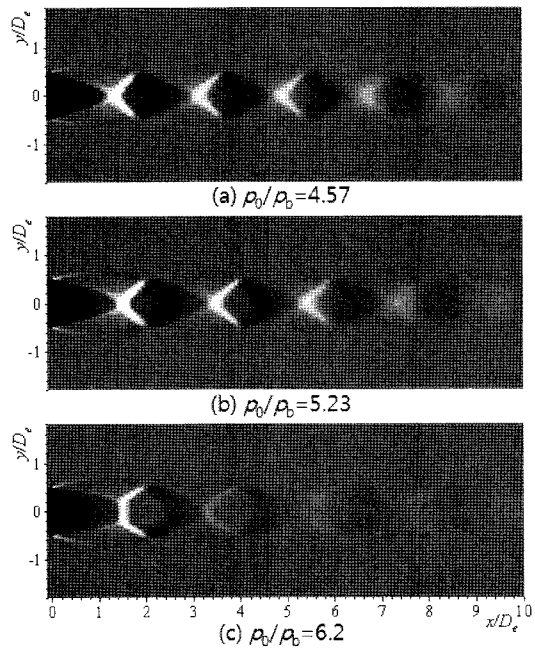

Fig. 4. Numerical schlieren images of 200 μm microjets

larger jets operating at higher Reynolds number as well as for supersonic microjets[3),7)].

The jet is in moderately underexpanded condition, at lower nozzle pressure ratio p_0/p_b, the

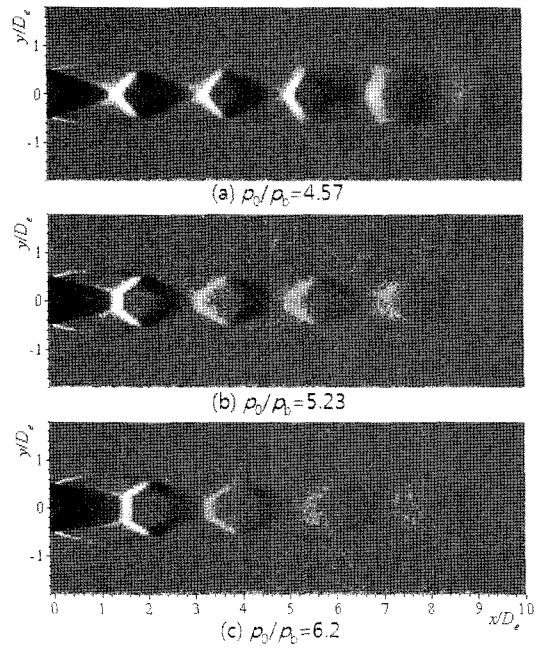

Fig. 5. Numerical schlieren images of 400 μm microjets

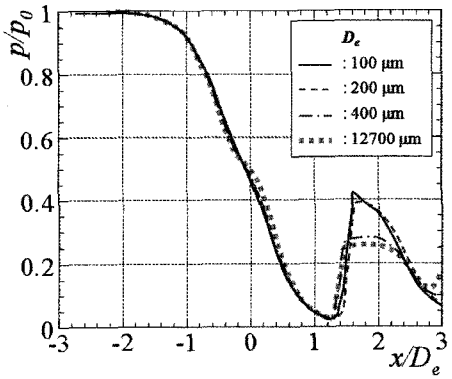

Fig. 6. Static pressure distributions along jet axis (p_0/p_b = 5.23)

oblique shocks almost crosses on the jet axis. However, as the jet underexpansion ratio increases, central Mach disk appears near the jet axis. The presence of such Mach disks is clearly visible in Figs. 3(c), 4(c) and 5(b, c). At triple-point the oblique shock, the Mach disk, and the rear shock are confluences and leads to a characteristic lambda (λ) shock structure. The velocity difference between the fluid streams that pass above and below this triple-point results in a shear layer or slip line. These slip lines emanating from the triple-point can be seen in Figs. 3(c), 4(c) and 5(b, c). Similar underexpanded flow features in supersonic microjets of 600 μm and 1,200 μm in diameter has been observed by Scroggs and Settles[3]. These features are also similar to larger jets operating at much higher Reynolds numbers.

4.3 Properties of Underexpanded Microjets

4.3.1 Surveys of Jet Centerline Pressure

The static pressure distributions downstream of the nozzle exit are strongly dependent on the nozzle exit diameter i.e. on jet diameter. This fact can be confirmed from the numerically predicted static pressure distributions along jet centerline at a nozzle pressure ratio of 5.23 in Fig. 6. The location of the sharp jump in the static pressure distribution is slightly varied with the jet diameter.

The centerline static pressure distributions for the 200 μm and 400 μm jets, are presented in Figs. 7(a) and (b), respectively. The pressures under each operating condition (p_0/p_b) exhibit unique charac-

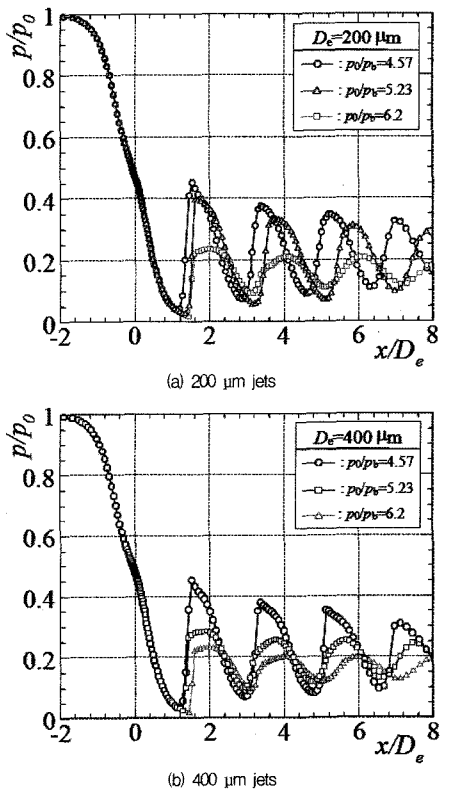

Fig. 7. Effect of nozzle pressure ratio on the static pressure distributions along jet axis

teristics. From Fig. 7(a), the variation in pressure shows the characteristic quasi-periodic structure, due to the presence of shock cells in the jet flow fields. Moreover, as the nozzle pressure ratio p_0/p_b is increased, the flow field is seen to stretch, where the shock cell spacing increases, leading to an increase in the length over which the shocks are present. At low p_0/p_b, the oblique shocks cross in a normal fashion, which changes to irregular crossing as the p_0/p_b is increased.

For 400 μm jet, the centerline pressure distributions displays characteristics very similar to 200 μm jet, as shown in Fig. 7(b). Furthermore, from Figs. 7(a) and (b), when the highly underexpanded condition is reached ($p_0/p_b = 6.2$), a Mach disk is first visually observed at the end of the first shock cell. At downstream of the first shock cell, the flow become subsonic, leading to a sudden drop in the pressure. The formation of Mach disk can also be clearly seen from the computer schlieren, in Figs. 3, 4 and 5.

4.3.2 Properties of Jet Structure

The configuration of jet boundary and barrel shock for different jet diameters at a nozzle pressure ratio of $p_0/p_b = 5.23$ is shown in Fig. 8. The locations of jet boundary and barrel shock were defined with the greatest value of density gradient (d_ρ/d_y) on an arbitrary cross section normal to x-axis. For a given nozzle pressure ratio, the jet diameter exhibits no significance influence on the configuration of jet boundary. However, the present

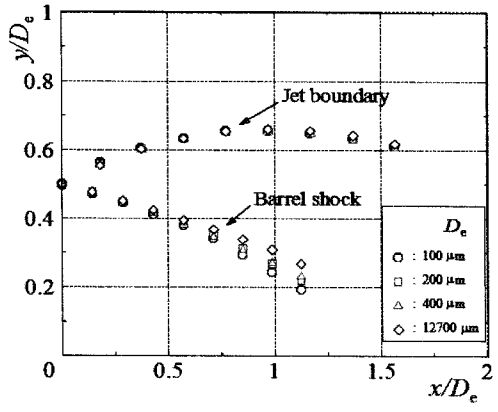

Fig. 8. Effect of nozzle exit diameter on jet boundary and barrel shocks ($p_0/p_b = 5.23$)

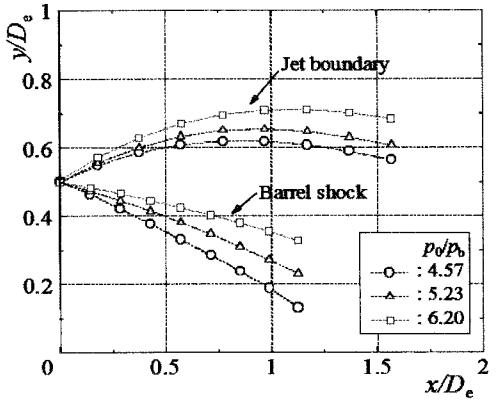

Fig. 9. Effect of nozzle pressure ratio on jet boundary and barrel shocks ($D_e = 400$ μm)

data shows a trend of outward expansion of barrel shock with the increase in jet diameter.

Figure 9 shows the configuration of jet boundary and barrel shock for 400 μm jet at nozzle pressure ratio of $p_0/p_b = 4.57$, 5.23 and 6.2. From this figure, boundary and barrel shock are significantly it is found that both the configuration of jet boundary and barrel shock are significantly influenced by the nozzle pressure ratio p_0/p_b and the jet is expanded outward with the nozzle pressure ratio p_0/p_b.

4.3.3 Properties of Shock Structure

The relation between the diameter D_m of Mach disk for the present microjets and the nozzle pressure ratio p_0/p_b is shown in Fig. 10, where the present computational results of microjets are compared with large-scale jet. As seen from Fig. 10, for

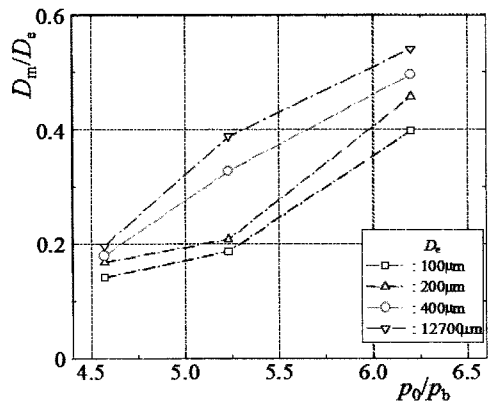

Fig. 10. Variation of Mach disk diameter with nozzle pressure ratio, p_0/p_b

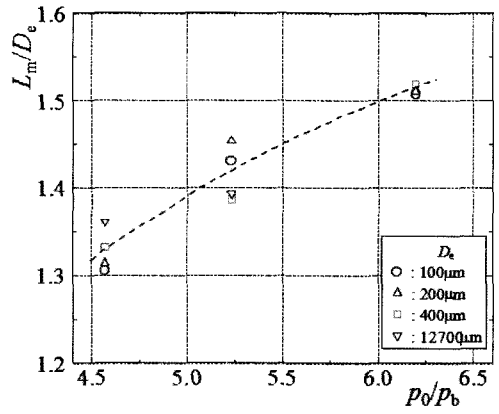

Fig. 11. Variation of Mach disk location with nozzle pressure ratio, p_0/p_b

different jet diameters, the diameter of Mach disk is an increasing function of the pressure ratio. It is also noted that for a given pressure ratio, the Mach disk diameter is significantly influenced by the jet diameter.

Figure 11 shows the relation between the location L_m of Mach disk from the nozzle exit and the nozzle pressure ratio p_0/p_b. It is found that the Mach disk location L_m is given by a function of the pressure ratio (p_0/p_b) and it is not so sensitive to the jet diameter, unlike the Mach disk diameter.

4.3.4 Surveys of Cross Stream Pressure

The cross-stream static pressure variations at different axial location of jet are examined under each operation condition (p_0/p_b). Cross-stream pressure profiles for 400 μm jet with the nozzle pressure ration of $p_0/p_b = 6.2$, which are the representative of other conditions, at axial locations of $x/D_e = 0.5$, 2.0 and 4.0 are shown in Fig. 12. Initially, at $x/D_e = 0.5$, the pressure profile exhibits a central peak, which is mainly due to the expansion fan located just after the nozzle exit. At the axial location just after the Mach disk, at $x/D_e = 2.0$, central depression is shown in the pressure profile due to the flow becoming subsonic. Further away from the nozzle exit, at $x/D_e \geq 4.0$, the shape of the pressure profile relaxes back to the central peak profile because of the weaker shock cells and shear layers merge.

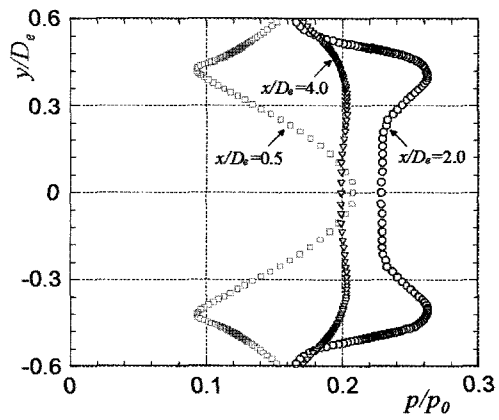

Fig. 12. Cross-stream pressure profiles at different axial locations (p_0/p_b = 6.2, D_e = 400 μm)

5. Conclusions

In the present study, axisymmetric supersonic microjets flow was investigated numerically under different operating conditions (p_0/p_b). Aerodynamic features of the jet flow field were compared with experimental results. Results obtained are summarized as follows: The presence of shock cells in the jet flow fields exhibit the characteristic quasi-periodic structure in the jet centerline pressure distributions. Moreover, at highly underexpanded condition, the Mach disks can be clearly visualized at the end of the first shock cell and the jet flow field is seen to stretch, where the shock cell spacing increases. For a given pressure ratio, the nozzle exit diameter has a significant influence on the configuration of barrel shock and the diameter of Mach disk. Other hand, the configuration of jet boundary and the location of Mach disk is not so sensitive to the nozzle exit diameter, for a given p_0/p_b. However, significant influence was observed on the configuration of jet boundary and barrel shock under different operating conditions (p_0/p_b), and the microjet is expanded outward with p_0/p_b.

References

1) Meinhart, C. D., Zhang, H., 2000, "The Flow Structure Inside a Microfabricated Inkjet Printhead", Journal of Microelectro- mechanical Systems, Vol.9, No.1.

2) Bayt, R. and Breuer, K., 1998, "Viscous Effects in Supersonic MEMS-Fabricated Micronozzles", Proceedings of the 3rd ASME Microfluids Symposium.
3) Scroggs, S. D. and Settles, G. S., 1996, "An Experimental Study of Supersonic Microjets" Experiments in Fluids, Vol.21.
4) Smedley, G. T., Phares, D. J. and Flagan, R. C., 1999, "Entrainment of fine particles from surfaces by impinging shock waves" Experiments in Fluids, Vol.26.
5) Krothapalli, A., Alvi, F. S., and Shih, C., 2001, "Behavior of Free and Impinging Supersonic Microjets", AIAA Paper 2001-3047.
6) Vela´squez-Aguilar, J. G., Toker, G., Zamudio-Lara, A., and Arias-Estrada, M., 2007, "Visualization of a supersonic air micro jet by methods of dual-holo- gram interfero- metry", Experiment in Fluids, Vol.42.
7) Phalnikar, K. A., Kumar, R. and Alvi, F. S., 2008, "Experiments on free and impinging supersonic microjets", Experiment in Fluids, Vol.44.
8) Goldberg, U. C., 1994, "Toward a Pointwise Turbulence Model for Wall-Bounded and Free Shear Flows", Transactions of the ASME, Vol.116, pp.72-76.
9) Yee, H. C., 1989, "A class of high-resolution explicit and implicit shock capturing methods", NASA TM-89464.
10) Addy, A. L., 1981, "Effects of Axisymmetric Sonic Nozzle Geometry on Mach Disk Characteri- stics", AIAA Journal, Vol.19, No.1.